

ARTICLE

Identification of Molecular Pathway Aberrations in Uterine Serous Carcinoma by Genome-wide Analyses

Elisabetta Kuhn, Ren-Chin Wu, Bin Guan, Gang Wu, Jinghui Zhang, Yue Wang, Lei Song, Xiguo Yuan, Lei Wei, Richard B.S. Roden, Kuan-Tin Kuo, Kentaro Nakayama, Blaise Clarke, Patricia Shaw, Narciso Olvera, Robert J. Kurman, Douglas A. Levine, Tian-Li Wang, le-Ming Shih

Manuscript received January 02, 2012; revised July 11, 2012; accepted July 16, 2012.

Correspondence to: le-Ming Shih, MD, PhD, Johns Hopkins Medical Institutions, 1550 Orleans Street, Rm 305, CRB2, Baltimore, MD 21231 (e-mail: ishih@jhmi.edu) and Tian-Li Wang, PhD, Johns Hopkins Medical Institutions, 1550 Orleans Street, Rm 306, CRB2, Baltimore, MD 21231 (e-mail: tlw@jhmi.edu).

Background Uterine cancer is the fourth most common malignancy in women, and uterine serous carcinoma is the most aggressive subtype. However, the molecular pathogenesis of uterine serous carcinoma is largely unknown. We analyzed the genomes of uterine serous carcinoma samples to better understand the molecular genetic characteristics of this cancer.

Methods Whole-exome sequencing was performed on 10 uterine serous carcinomas and the matched normal blood or tissue samples. Somatic acquired sequence mutations were further verified by Sanger sequencing. The most frequent molecular genetic changes were further validated by Sanger sequencing in 66 additional uterine serous carcinomas and in nine serous endometrial intraepithelial carcinomas (the preinvasive precursor of uterine serous carcinoma) that were isolated by laser capture microdissection. In addition, gene copy number was characterized by single-nucleotide polymorphism (SNP) arrays in 23 uterine serous carcinomas, including 10 that were subjected to whole-exome sequencing.

Results We found frequent somatic mutations in *TP53* (81.6%), *PIK3CA* (23.7%), *FBXW7* (19.7%), and *PPP2R1A* (18.4%) among the 76 uterine serous carcinomas examined. All nine serous carcinomas that had an associated serous endometrial intraepithelial carcinoma had concordant *PIK3CA*, *PPP2R1A*, and *TP53* mutation status between uterine serous carcinoma and the concurrent serous endometrial intraepithelial carcinoma component. DNA copy number analysis revealed frequent genomic amplification of the *CCNE1* locus (which encodes cyclin E, a known substrate of *FBXW7*) and deletion of the *FBXW7* locus. Among 23 uterine serous carcinomas that were subjected to SNP array analysis, seven tumors with *FBXW7* mutations (four tumors with point mutations, three tumors with hemizygous deletions) did not have *CCNE1* amplification, and 13 (57%) tumors had either a molecular genetic alteration in *FBXW7* or *CCNE1* amplification. Nearly half of these uterine serous carcinomas (48%) harbored *PIK3CA* mutation and/or *PIK3CA* amplification.

Conclusion Molecular genetic aberrations involving the p53, cyclin E–*FBXW7*, and PI3K pathways represent major mechanisms in the development of uterine serous carcinoma.

J Natl Cancer Inst 2012;104:1503–1513

Endometrial carcinoma is the most frequently diagnosed gynecological cancer and the fourth most common malignant neoplasm among women in the United States (1). Traditionally, endometrial carcinoma is classified into two main groups: type I and type II (2). Type I endometrial carcinoma is composed of low-grade endometrioid carcinoma, and type II is composed mainly of uterine serous carcinoma. Uterine serous carcinoma occurs in older women and often presents at an advanced stage. Low-grade endometrioid carcinomas are estrogen dependent and develop from endometrial hyperplasia, whereas uterine serous carcinomas are estrogen independent and arise in atrophic endometrium and endometrial polyps from preinvasive lesions known as serous endometrial

intraepithelial carcinoma. Although uterine serous carcinomas constitute only 10% of all endometrial cancers, they account for a disproportionately high number of deaths (3). This highly aggressive behavior is related mainly to the unique tendency of uterine serous carcinomas to metastasize even when the primary tumor is small; as a result, most patients with uterine serous carcinoma have metastatic disease, which is not curable, at the time of diagnosis. Moreover, uterine serous carcinoma is highly resistant to conventional chemotherapy, and recurrence is inevitable in most patients with advanced-stage disease. Until the molecular pathogenesis of uterine serous carcinoma is better understood, therapeutic interventions to improve the clinical outcomes of these patients remain empirical.

Previous molecular genetic studies of endometrial carcinoma have focused on low-grade endometrioid carcinoma (4,5). More recently, the genome-wide molecular changes in endometrioid carcinomas, especially those of low grade, have been revealed through the efforts of The Cancer Genome Atlas (TCGA; <https://tcgadata.nci.nih.gov/tcga/tcgaCancerDetails.jsp?diseaseType=UCEC&diseaseName=Uterine%20Corpus%20Endometrioid%20Carcinoma>). By contrast, the molecular genetic changes that account for the malignant behavior of uterine serous carcinoma are largely unknown. Thus, the purpose of this study is to elucidate the molecular genetic characteristics of uterine serous carcinoma by cataloguing the genetic alterations detected by whole-exome sequencing and gene copy number analysis, with emphasis on identifying the aberrant molecular pathways that may be targetable for therapeutic intervention.

Methods

Tissue Specimens and Genomic DNA Preparation

A total of 76 uterine serous carcinomas were studied in this report: six fresh tumors from which we affinity purified tumor cells (designated by the suffix “TS” or “S”) and four frozen tumors (designated by the suffix “T”) were used for discovery, and 66 tumors including 34 frozen tumors and 32 paraffin-embedded tumors were used for validation. Normal tissues were designated with the suffix “N.” The diagnosis of uterine serous carcinoma was confirmed in all tumors according to previously described diagnostic criteria (6,7) by three gynecological pathologists (EK, RJK, I-MS) based on review of the hematoxylin and eosin–stained slides. The tumor cells from the six of the 10 specimens in the discovery set were isolated by digestion with collagenase I (Roche, Indianapolis, IN), followed by epithelial cell enrichment using Dynalbeads coated with EpCAM antibodies (Invitrogen Inc., Carlsbad, CA). We performed immunocytochemistry using an anti-cytokeratin antibody (prediluted, CAM5.2; Becton Dickinson, Franklin Lakes, NJ) to ensure that more than 90% of cells in the purified samples were epithelial cells. Affinity purification of tumor cells and immunocytochemistry were performed as previously described (8,9). Genomic DNA was extracted from both tumor and normal cells with the use of a DNeasy Blood and Tissue kit (Qiagen, Inc., Valencia, CA) according to the manufacturer’s protocol.

The validation set comprising 66 uterine serous carcinomas was obtained from the Johns Hopkins Hospital (Baltimore, MD), Memorial Sloan-Kettering Cancer Center (New York, NY), and University of Toronto Health System (Toronto, ON, Canada). Among tumors from discovery and validation sets, nine contained serous intraepithelial carcinoma, a preinvasive (in situ) uterine serous carcinoma component, which was isolated by laser-capture microdissection. Genomic DNA was isolated from all validation set samples as described above and was subjected to Sanger sequencing analysis. Patient consent information was not available because we used anonymous tissue materials that lacked patient’s identification. The use of de-identified tissue material was approved by the Institutional Review Boards of Johns Hopkins Hospital, Memorial Sloan-Kettering Cancer Center, University of Toronto Health System, and the National Taiwan University Hospital.

Whole-Exome Sequencing of the Discovery Set

Exome DNA capture was performed with the use of a TruSeq Exome Enrichment Kit (Illumina, San Diego, CA), and paired-end libraries were constructed with the use of a TruSeq DNA Sample Prep Kit (Illumina) as previously described (7). Paired-end sequencing (100-bp reads × 2) was performed with the use of a HiSeq Analyzer (Illumina) provided by Illumina’s Fast Track genetic analysis service. Whole-exome sequencing was also performed on DNA isolated from the matched normal tissues (peripheral mononucleated blood cells or myometrium) from each of the 10 patients who had tumor tissue in the discovery set.

All Illumina paired-end reads from both tumor and matched normal DNA were aligned to the human reference sequence known as the National Center for Biotechnology Information (NCBI) Build 36 (ftp://ftp.ncbi.nih.gov/genomes/H_sapiens/ARCHIVE/BUILD.36.3/) using the Burrows–Wheeler Aligner (version 0.5.5) (10), and reads were removed using the Picard package 1.29 (<http://picard.sourceforge.net>). The total number of sequencing reads and mapping statistics were assessed by using the flagstat function of samtools (version 0.1.7) (10).

The effective coverage of the whole exome was obtained by summarizing the coverage of aligned bases using the Coverage module of Bambino. We only included sequencing reads with a quality score of 15 or higher so that the expected error rate was less than 5% at each position of the reference human exome (11). We considered a base as covered if the effective coverage was at least 10-fold. We also excluded all ambiguous bases and sequencing gaps in the human reference sequence from our coverage analysis. The exome annotation was based on NCBI RefSeq (12).

Detection of Somatic Sequence Mutations

Putative sequence mutations, including single-nucleotide variations, insertions, or deletions, were initially detected by using the variation detection module of Bambino (11). Specifically, the analysis was run using three different parameters as previously described (13,14): a) a high-quality threshold (minimum quality score set to 20) for pooled tumor and matching normal tissue BAM files; b) a low-quality threshold (minimum quality score set to 10) for pooled tumor and matching normal tissue BAM files; and c) a high-quality threshold (minimum quality score set to 20) for normal tissue-only analysis (see definition of minimum quality score at <https://cgwb.nci.nih.gov/goldenPath/bamview/documentation/index.html>). The pooled tumor–normal tissue analysis reduces the possibility of misclassifying germline variations with poor coverage in matching normal tissue samples as somatic mutations. Variants identified by normal tissue-only analysis were removed for further consideration, whereas those only identified by paired tumor and normal tissue analysis were subjected to an automated review process to remove additional false-positive calls caused by misalignment or mismapping of whole-exome sequencing reads. Specifically, the automated review process firstly used the Smith–Waterman algorithm to realign all reads that harbored the mutant allele, followed by quality and alignment trimming, then a double-strand coverage check for the variant allele, and a final remapping of reads that harbored the minor allele to the reference genome to ensure uniqueness.

Transcripts from NCBI RefSeq (build download May 21, 2009) (12) were used for annotation. Variants were classified as coding synonymous ("silent"), missense, nonsense, intronic, regions within 10bp of a canonical splice site, splice site, or noncoding RNA variants, as well as those that occurred in 3' and 5' untranslated regions. The insertions and deletions were further classified as frameshifts or in-frame insertions or deletions.

Analysis of Background Mutation Frequency

Assuming that the silent codon position is selectively neutral, we used the mutation rate at this position to approximate the background mutation frequency. Specifically, the background mutation frequency (μ) can be calculated by the following equation:

$$\mu = \frac{M}{\beta * N_e},$$

where M is the total number of validated silent somatic mutations in each tumor sample (ie, the nonfunctional background mutations), N_e is the total number of effectively covered coding bases (ie, simultaneously covered by ≥ 10 -fold in both tumor and matching normal tissue) in all RefSeq protein coding genes, and β is the silent-to-nonsilent ratio [estimated to be 0.350 by the TCGA Consortium (15)] across the coding regions.

Sanger Sequencing for Validation of Putative Mutations

Putative mutations identified by whole-exome sequencing were validated by conventional Sanger sequencing of both tumor and normal DNA (from peripheral blood mononucleated cells or myometrium) samples in the discovery set. Before Sanger sequencing, genomic DNA containing the putative mutations was amplified by polymerase chain reaction (PCR) with the use of primers that flanked the putative mutations. We also used the Sanger method to sequence DNA isolated from the 66 uterine serous carcinomas and matched normal tissue in the validation set to identify the prevalence of somatic mutations in selected genes. The results of Sanger sequencing were analyzed using Mutation Surveyor software (version 4.0; SoftGenetics, State College, PA).

Single-Nucleotide Polymorphism Array and DNA Copy Number Analysis

We analyzed 23 uterine serous carcinomas for which there was sufficient material to examine DNA copy number changes by single-nucleotide polymorphism (SNP) arrays. These included 10 samples from the discovery set and 13 frozen tumors from the validation set. SNPs were genotyped using 250K *StyI* arrays (seven tumors) or SNP Array 6.0 (16 tumors; both arrays from Affymetrix, Santa Clara, CA) at the Microarray Core Facility at the Johns Hopkins University according to manufacturer's instructions. In addition, 13 uterine endometrioid carcinomas from the National Taiwan University Hospital were analyzed for copy number alterations using the 250K *StyI* arrays. The SNP array data for 25 normal tissues, 12 ovarian serous borderline tumors, 12 ovarian low-grade serous carcinomas, seven ovarian endometrioid carcinomas, 12 ovarian clear cell carcinomas, and 33 ovarian high-grade serous carcinomas were previously reported (16,17).

The analysis of SNP array data was performed using the dChip software (2006 version) as previously described (16,17). Only data corresponding to probes present in both SNP Array 6.0 and 250K *StyI* array were analyzed. To quantify the relative levels of somatic DNA copy number alterations, we used a previously described method (17) to calculate the genome-wide chromosomal instability index based on dChip analysis to infer the copy number. To identify the genes and regions with somatic copy number alterations (DNA copy number gain or loss as compared with matched normal tissue samples), the intensity of each probe was inferred with the use of Genotyping Console software (version 4.1.3; Affymetrix). To detect somatically altered chromosomal regions in the 23 uterine serous carcinomas, we used R package DNACopy (<http://www.bioconductor.org/packages/2.3/bioc/html/DNACopy.html>) to perform circular binary segmentation analysis (18,19) and combined the segmentation results for all 23 uterine serous carcinomas. To identify the genes with statistically significant DNA copy number alterations, we used cghMCR (<http://www.bioconductor.org/packages/2.3/bioc/html/cghMCR.html>), an R implementation of a modified version of GISTIC analysis (20), because the original GISTIC algorithm only works for segmentation results from the same platform. Instead of the G score, which is reported by GISTIC algorithm, the cghMCR package uses a Segments-of-Gain-Or-Loss (SGOL) score to indicate the frequency and degree of copy number changes in each gene or segment. Here, we selected three standard deviations (SDs) from the mean SGOL score as the cutoff because 99.7% of genes had SGOL scores within this range. In particular, we defined amplified genes as the genes with SGOL scores greater than 3 SDs of the mean SGOL scores and deleted genes as those with SGOL scores less than 3 SDs of the mean SGOL scores.

Immunohistochemistry

Immunohistochemistry for p53 and cyclin E1 expression was performed on paraffin-embedded sections of 41 and 37 uterine serous carcinomas, respectively, from both the validation and discovery sets. The detailed protocol for p53 immunohistochemistry has been reported previously (21). Briefly, after antigen retrieval was carried out with Cell Conditioning 1 solution (Ventana Medical Systems, Tucson, AZ), the sections were incubated with a mouse monoclonal p53 antibody (clone Bp53-11, prediluted; Ventana Medical Systems) for 16 minutes at 37°C. Staining was detected with the use of an iView DAB detection system (Ventana Medical Systems). For cyclin E1 staining, heat-induced epitope retrieval was performed with the use of Target Retrieval Solution (Dako, Carpinteria, CA), and nonspecific endogenous peroxidase activity was blocked by treatment with 3% hydrogen peroxide. The sections were then incubated with a polyclonal rabbit cyclin E antibody (1:250 dilution; Sigma-Aldrich, St Louis, MO) at room temperature for 65 minutes, followed by antibody detection with the use of an LSAB kit (catalog # K0690; Dako). Cyclin E1 immunoreactivity was visualized by a peroxidase reaction (Dako), and the sections were counterstained with hematoxylin (Dako).

Chromosomal Instability Index Analysis

We used the genome-wide chromosomal instability index to quantify the degree of somatic DNA copy number alterations according

to a previously described method (17). The genome-wide chromosomal instability index was defined as $\log(C1 + 1) + \dots + \log(Ci + 1) + \dots + \log(C23 + 1)$, where $C1$, Ci , and $C23$ are the chromosomal instability indices for chromosomes 1, i , and 23, respectively. The chromosomal instability index for each chromosome was calculated as the sum of magnitudes of all subchromosomal segments whose copy numbers were amplified or deleted. The magnitude of an amplified copy number segment was the average intensity of SNP signals within the segment. The magnitude of a deleted copy number segment was normalized by the transformation $2.5 + (R - 2.5)(1.5 - x)/1.5$, where x was the average intensity of SNP signals within the segment and R was the maximum magnitude of amplified copy number segments across all samples.

Statistical Analysis

We used one-way analysis of variance (ANOVA) followed by the Tukey–Kramer test for multiple comparisons to examine whether the chromosomal instability index for uterine serous carcinoma was statistically significantly higher than that for other types of gynecological neoplastic diseases based on our previous report (17). The Fisher exact test was used to compare the frequency of somatic mutations of several candidate genes in uterine serous carcinoma with the previously reported frequency in high-grade serous carcinoma of the ovary (22); P values were adjusted using the Bonferroni method. The association between p53 immunopositivity and *TP53* mutation status was evaluated by a two-tailed Fisher exact test. All statistical tests were two-sided, and a P value less than .05 was considered statistically significant.

Results

Paired-End Whole-Exome Sequencing of Uterine Serous Carcinoma

To gain new insight into the genetic basis of uterine serous carcinoma, we determined the sequences of approximately 18 000 protein-encoding genes in tumor and normal tissue samples from 10 uterine serous carcinomas by paired-end sequencing. To increase the sensitivity of somatic mutation detection, we used DNA extracted from epithelial tumor cells that were affinity-purified from six fresh tumor specimens with the use of EpCAM antibody-conjugated beads. Immunohistochemical staining of the purified cells with a cytokeratin antibody verified that more than 90% of each tumor was of epithelial origin. Our use of a high-throughput, paired-end sequencing system resulted in more than 75 million reads per DNA sample. The mean mapping rate for total reads was 98.4% (SD = 0.4%), and the mean percentage of targeted bases that were covered by at least 10 reads was 89.9% (SD = 2.5%) (Supplementary Table 1, available online). We identified 946 somatic mutations in 874 genes among 10 uterine serous carcinomas using the method reported in the analysis of whole genome sequencing data of T-cell precursor acute lymphoblastic leukemia and retinoblastoma (13,14). To ensure that our method could reliably detect somatic mutations, we resequenced 331 randomly selected mutated regions (mainly those containing nonsilent mutations) by Sanger sequencing and verified that 303 (91.5%) contained the originally identified mutation (Supplementary Table 2, available online).

The median number of somatic sequence mutations for uterine serous carcinomas in the discovery set, including synonymous and nonsynonymous changes, alterations in 5' and 3' untranslated regions, and alterations in noncoding RNA, was 96 (range = 38–156) (Supplementary Table 3, available online). The median number of somatic nonsynonymous and splice site mutations for uterine serous carcinomas in the discovery set was 38 (range = 10–64). The most common sequence mutation in these 10 uterine serous carcinomas was a C to T or G to A transition (Supplementary Figure 1, available online). Specifically, there were 454 nonsynonymous and splice site mutations in 425 genes (Supplementary Table 2, available online), and the average nonsilent-to-silent mutation ratio was 3:2 (Supplementary Table 3, available online). Among the 425 somatically mutated genes, 14 were mutated in two or more of the 10 uterine serous carcinomas: *TP53*, *PIK3CA*, *FBXW7*, *PPP2R1A*, *BSN*, *DNAH11*, *NEB*, *OBSCN*, *ORAI2*, *RNF19B*, *SLC28A1*, *SPTA1*, *UBA2*, and *UTRN* (Table 1). To identify other cancer-related genes that are less commonly mutated in uterine serous carcinoma, we compared all genes harboring mutations from this study with the cancer-related mutations reported in the Cancer Gene Census database (<http://www.sanger.ac.uk/genetics/CGP/Census/>). This comparison yielded 16 genes: four genes (*FBXW7*, *PIK3CA*, *PPP2R1A*, and *TP53*) were mutated in more than one of the 10 uterine serous carcinomas, whereas 12 cancer-associated genes occurring in Cancer Gene Census database were mutated only once in these 10 tumors (*AKAP9*, *BCL9*, *BRCA2*, *ERCC5*, *KRAS*, *LHFP*, *MLL3*, *MYH11*, *NCOA2*, *NSD1*, *PDGFRA*, and *USP6*). Of note, all three missense mutations detected in *FBXW7* occurred at the Arg465 hotspot (COSMIC database, <http://www.sanger.ac.uk/perl/genetics/CGP/cosmic?action=bygene&ln=FBXW7&start=1&end=708&coords=AA:AA>), whereas none of the four *PIK3CA* mutations were located at previously reported exons containing hotspots. We found no mutations in mismatch repair genes in any of the 10 tumors in the discovery set.

Prevalence Screening of Mutations in Selected Genes

We performed Sanger sequencing to determine prevalence of mutations in *FBXW7*, *FBXW8*, *PIK3CA*, *PPP2R1A*, *PIK3C2B*, *PIK3R4*, *RNF19B*, and *TP53* in 34 frozen tumors from the validation set with sufficient DNA. In addition, we sequenced known mutational hotspots in *FBXW7* [coding exons 8 and 9; (23)], *PIK3CA* [coding exons 1, 9, and 20; (24)], *PPP2R1A* [coding exons 5 and 6; (25)], and *TP53* (coding exons 4–9; COSMIC database, <http://www.sanger.ac.uk/perl/genetics/CGP/cosmic?action=bygene&ln=TP53&start=1&end=394&coords=AA:AA>) in an additional 32 paraffin-embedded uterine serous carcinomas from the validation set. We also sequenced exon 9 of *FBXW8* in the 32 uterine serous carcinomas because a somatic mutation in this exon was identified in our discovery screen. *RNF19B* was selected for validation because it was somatically mutated in two of the 10 uterine serous carcinomas in the discovery set and it encodes an E3 ligase that ubiquitinates uridine-cytidine kinase-like 1 (UCKL1), a tumor survival factor (26–28). Although only one somatic mutation was found in the discovery set for *FBXW8*, *PIK3C2B*, and *PIK3R4*, these genes were chosen for validation because, similar to *FBXW7*, *FBXW8* also contains F-box and

Table 1. Recurrently mutated genes in 10 uterine serous carcinomas of the discovery set*

Gene	Transcript	900T	366TS	702TS	863TCS	340TS	993TCS	FM403T	DM851T	FM474T	555TS	Total
<i>TP53</i>	NM_000546.4	c.677del p.G226Afs		c.742C>T p.R248W c.1252G>A p.E418K	c.722C>T p.S241F c.353G>A p.G118D	c.481G>A p.A161T	c.832C>A p.P278T	c.647_672+3del p.V216Gfs c.1093G>A p.E365K	c.713G>A p.C238Y	c.742C>T p.R248W c.1031T>G p.V344G	c.730G>C p.G244R	9
<i>PIK3CA</i>	NM_006218.2											4
<i>FBXW7</i>	NM_033632.2	c.1393C>T p.R465C	c.1394G>A p.R465H						c.1394G>T p.R465L			3
<i>PPP2R1A</i>	NM_014225.3			c.767C>A p.S256Y							c.536C>G* p.P179R*	2
<i>BSN</i>	NM_003458.3		c.8374C>G p.Q2792E		c.2687G>A p.R896H							2
<i>DNAH11</i>	NM_003777.3	c.3925G>A p.A1309T						c.6536T>C p.V2179A c.23491A>T p.I7831F				2
<i>NEB</i>	NM_001164508.1											2
<i>OBSN</i>	NM_001098623.1					c.20330T>C p.V6777A c.11274_11275del p.H3758Qfs					c.22967A>T p.E7656V	2
<i>ORAI2</i>	NM_001126340.1								c.214G>A p.G72S	c.397T>G p.S133A		2
<i>RNF19B</i>	NM_153341.2			c.842-5C>G ex3_splice				c.1264G>T p.G422C c.1754G>A p.C585Y				2
<i>SLC28A1</i>	NM_004213.3											2
<i>SPTA1</i>	NM_003126.2	c.610del p.Q204Kfs							c.-16-1G>T ex3_splice c.3697G>A p.V1233I			2
<i>UBA2</i>	NM_005499.2			c.347T>C p.L116S						c.223-2A>T ex3_splice c.5074-1G>A ex36_splice		2
<i>UTRN</i>	NM_007124.2				c.8782G>A p.V2928I							2

* Sanger sequencing discovered an additional *PPP2R1A* mutation that was not originally recorded in the Illumina HiSeq platform.

WD-40 domains and functions as E3 ubiquitin ligase (29), and both *PIK3C2B* and *PIK3R4* are involved in the phosphatidylinositol 3-kinase (PI3K) signaling pathway (30). The prevalence of somatic mutations in *TP53*, *PIK3CA*, *FBXW7*, and *PPP2R1A* in the validation set ($n = 66$) was 80.3%, 21.2%, 18.2%, and 18.2%, respectively. When we combined all uterine serous carcinomas from the discovery and validation sets ($n = 76$), the prevalence of somatic mutations in *TP53*, *PIK3CA*, *FBXW7*, and *PPP2R1A* was 81.6%, 23.7%, 19.7%, and 18.4%, respectively (Table 2); all mutations in these four genes in all 76 tumors are listed in Supplementary Table 4 (available online). For *FBXW7*, there were 16 somatic mutations (15 mutations involved the coding region and one involved the noncoding region at the splice site) detected in 15 tumors among all 76 tested tumors; all *FBXW7* somatic mutations involving the coding region occurred in the WD40 domain, whose function in E3 ubiquitin ligases is to recognize phosphorylated ubiquitination signals (31). However, we did not detect any somatic mutations in *FBXW8*, *PIK3C2B*, *PIK3R4*, or *RNF19B* in the validation set. It should be noted that the higher mutation frequency of *TP53* in the discovery set than in the validation set (90% vs 80%) may reflect the fact that we used affinity-purified tumor cells in some of the discovery samples. Accordingly, the actual prevalence of mutations in all the genes analyzed could be slightly higher than that reported in this study.

To examine whether the *TP53* mutation pattern was associated with p53 protein expression in carcinoma tissues, we performed p53 immunohistochemistry on 41 uterine serous carcinomas from both discovery and validation sets for which paraffin-embedded tissues were available. We found that 27 of 28 tumors bearing *TP53* missense mutations or in-frame deletion had diffuse p53 staining (data not shown). The frequency of diffuse staining in tumors with *TP53* missense mutation or in-frame deletion was statistically significantly higher than in those with a null mutation or wildtype *TP53* (96.4% vs 46.2%, $P < .001$, two-tailed Fisher exact test). These findings are consistent with our previous report showing a similar association between p53 immunostaining pattern and *TP53* mutation type in ovarian high-grade serous carcinomas and serous tubal intraepithelial carcinomas (21).

In contrast, by analyzing 316 ovarian high-grade serous carcinomas from the ovarian cancer dataset of TCGA [https://tcga-data.nci.nih.gov/docs/publications/ov_2011/; (22)], we found somatic mutations of *PIK3CA*, *FBXW7*, and *PPP2R1A* in only 0.63%, 0.95%, and 1.27%, respectively (Supplementary Table 5, available online). The mutation frequencies of those genes were statistically significantly higher in uterine serous carcinoma than in ovarian high-grade serous carcinoma ($P < .001$, Fisher exact test) (Supplementary Table 5, available online).

DNA Copy Number Alterations in Uterine Serous Carcinoma and Other Gynecological Cancers

Because DNA copy number alterations are commonly associated with tumorigenesis (32), we also used the SNP arrays for copy number analysis of 23 uterine serous carcinomas (10 from discovery set and 13 from validation set) for which the genomic DNA was available for analysis. By using the chromosomal instability index, a quantitative measure of the genome-wide level of DNA copy number changes (17), we found that among a panel of gynecological tumors, uterine serous carcinoma displayed a mean chromosomal instability index comparable to that of ovarian high-grade serous carcinoma, a fatal subtype of ovarian cancer with known prominent genomic alterations (Supplementary Table 6, available online) (17,22). The mean chromosomal instability index for both uterine serous carcinoma (mean = 1.129) and ovarian high-grade serous carcinomas (mean = 1.475) was statistically significantly higher than that in other types of gynecological cancers, including uterine endometrioid carcinoma (mean = 0.298), ovarian serous borderline tumor (mean = 0.134), ovarian low-grade serous carcinoma (mean = 0.386), ovarian endometrioid carcinoma (mean = 0.228), and ovarian clear cell carcinoma (mean = 0.302) ($P < .001$, one-way ANOVA followed by Tukey–Kramer test) (Figure 1, A and B). The details of the chromosome instability index for each type of gynecological cancer and P values for all pair-wise comparisons are shown in Supplementary Table 6 (available online).

DNA Copy Number Alterations in Uterine Serous Carcinoma

We used DNACopy and cghMCR software to identify genomic regions of uterine serous carcinomas that displayed a statistically significant copy number gain or loss compared with normal tissues. By using the mean SGOL score plus or minus 3 SDs to define amplified and deleted genes, respectively, we found 13 discrete amplified regions containing 307 genes and 25 discrete deleted regions containing 520 genes, including 25 regions that harbored six or fewer genes (Supplementary Tables 7 and 8, available online). Frequently amplified genes (and the corresponding chromosomal locations) included *BCL9* (1q21.1), *EVII* (3q26.2), *KRAS* (12p12.1), *ADAM6* (14q32.33), and *CCNE1* (19q12); the percentage of samples that exhibited an inferred gene copy number greater than three for *BCL9*, *EVII*, *KRAS*, *ADAM6*, and *CCNE1* were 13%, 21.7%, 4.4%, 30.4%, and 26.1%, respectively. Among these frequently amplified genes, the *CCNE1* locus (chromosome 19: nucleotide 34 995 401–35 007 059) demonstrated a very high SGOL score (9.1) and was amplified in six of the 23 uterine serous carcinoma samples examined (Figure 1, C and D). The most commonly deleted regions harbored *LCE3C* (1q21.3), *MGAM* (7q34), *CSMD1* (8p23.2), and *CDH13* (16q23.3); these deletions

Table 2. The prevalence of most common somatic mutations (frequency >10%) in uterine serous carcinoma in all 76 tumors analyzed

Sample set	No. of tumors analyzed	<i>FBXW7</i> mutation	<i>PIK3CA</i> mutation	<i>PPP2R1A</i> mutation	<i>TP53</i> mutation
Discovery set	10	3	4	2	9
Validation set (paraffin-embedded tissues)	32	8	5	4	24
Validation set (frozen tissues)	34	4	9	8	29
Total (%)	76 (100.0)	15 (19.7)	18 (23.7)	14 (18.4)	62 (81.6)

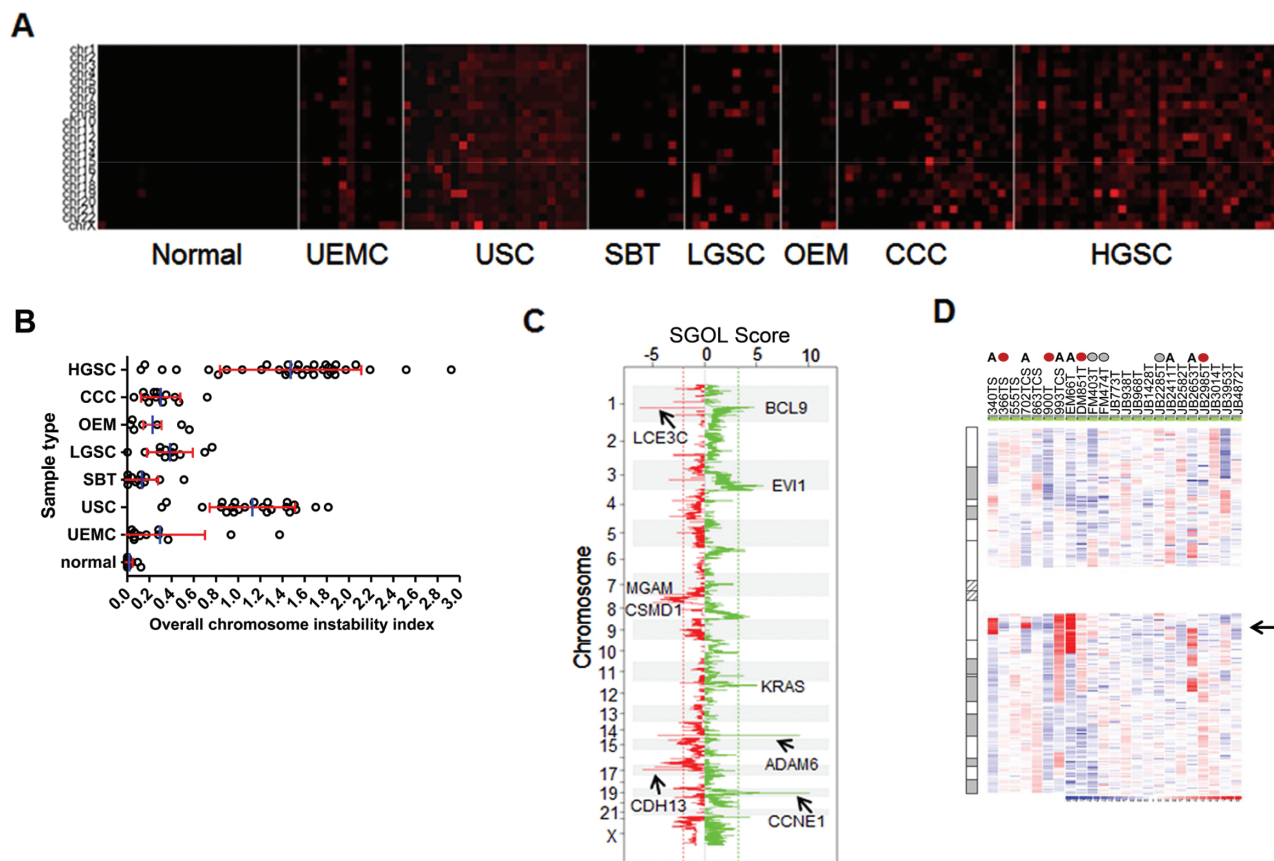


Figure 1. Single-nucleotide polymorphism array analysis of DNA copy number alteration. **A**) Copy number alteration in uterine serous carcinoma and other types of gynecological neoplasia. Individual chromosomes (vertical axis) of each tumor (horizontal axis) are plotted using a pseudocolor gradient indicating the overall level of copy number alteration (low [black] to high [red]). Normal = normal tissue (n = 25); UEMC = uterine endometrioid carcinoma (n = 13); USC = uterine serous carcinoma (n = 23); SBT = ovarian serous borderline tumor (n = 12); LGSC = ovarian low-grade serous carcinoma (n = 12); OEM = ovarian endometrioid carcinoma (n = 7); CCC = ovarian clear cell carcinoma (n = 12); HGSC = ovarian high-grade serous carcinoma (n = 33). **B**) Scatter plot of genome-wide chromosome instability index for individual tumors (open circles). Vertical blue lines indicate mean values; horizontal red lines indicate plus or minus one SD. **C**) Overall view of DNA copy number gain and loss in uterine serous carcinoma. To generate an overview of DNA copy number alterations, we performed circular binary segmentation analysis and combined the segmentation results for all 23 uterine serous carcinomas. Based on the Segments-of-Gain-Or-Loss (SGOL) scores (horizontal axis), DNA copy number gains (green) and losses (red) are plotted as a function of distance along the normal genome (vertical axis). Dashed vertical lines are generated based on the values of 3 SDs of the SGOL scores of gains or losses. Tumor-associated genes located in representative amplified and deleted regions are annotated. **D**) Heat map of DNA copy number ratio along the chromosome 19. Arrow shows amplification in the *CCNE1* locus in 23 uterine serous carcinoma samples. A = *CCNE1* amplification; red circles = *FBXW7* mutation; gray circle = *FBXW7* hemizygous deletion. Suffix of the tumor numbers: TS and TCS = fresh tumor with affinity-purified tumor cells; T = tumor samples without affinity purification; N = normal control.

occurred in 17.4%, 34.8%, 26.1%, and 34.8%, respectively, of the 23 uterine serous carcinomas.

To discover cancer-associated genes whose function was affected by somatic point mutation and DNA copy number change, we compared the genes that harbored nonsynonymous and splice site mutations (Supplementary Table 2, available online) with those that are amplified or deleted (Supplementary Tables 7 and 8, available online). This comparison yielded 11 genes, including *BCL9*, *DAZAP1*, and *KRAS* (Supplementary Table 9, available online). In addition, close examination of copy number at the *FBXW7* locus revealed that *FBXW7* was deleted in a hemizygous fashion in three tumors (Supplementary Figure 2, available online). This is interesting because *FBXW7* encodes a substrate recognition component of a SKP1-cullin-F-box (SCF)-type E3 ubiquitin ligase, which is responsible for ubiquitin-dependent degradation of cyclin E (encoded by *CCNE1*). Thus, we examined

the co-occurrence of somatic mutations and/or *FBXW7* deletion and *CCNE1* amplification in the 23 uterine serous carcinomas that were subjected to SNP array analysis. We found that seven tumors with *FBXW7* mutations (four tumors with sequence mutations, three tumors with hemizygous deletions) did not have *CCNE1* amplification, and six tumors with *CCNE1* amplification did not have *FBXW7* mutations; therefore, 13 (57%) of 23 tumors had either a molecular genetic alteration in *FBXW7* or *CCNE1* amplification (Figure 2, A). We also found that *PIK3CA* mutation and gene amplification were mutually exclusive except for one tumor (case ID: JB2411), which showed both genetic alterations. Integrated analysis demonstrated that 48% of the 23 uterine serous carcinomas harbored a *PIK3CA* mutation and/or *PIK3CA* amplification (Figure 2, A). Taken together, these findings suggest that the cyclin E-*FBXW7* and PI3K pathways are involved in the development of uterine serous carcinoma.

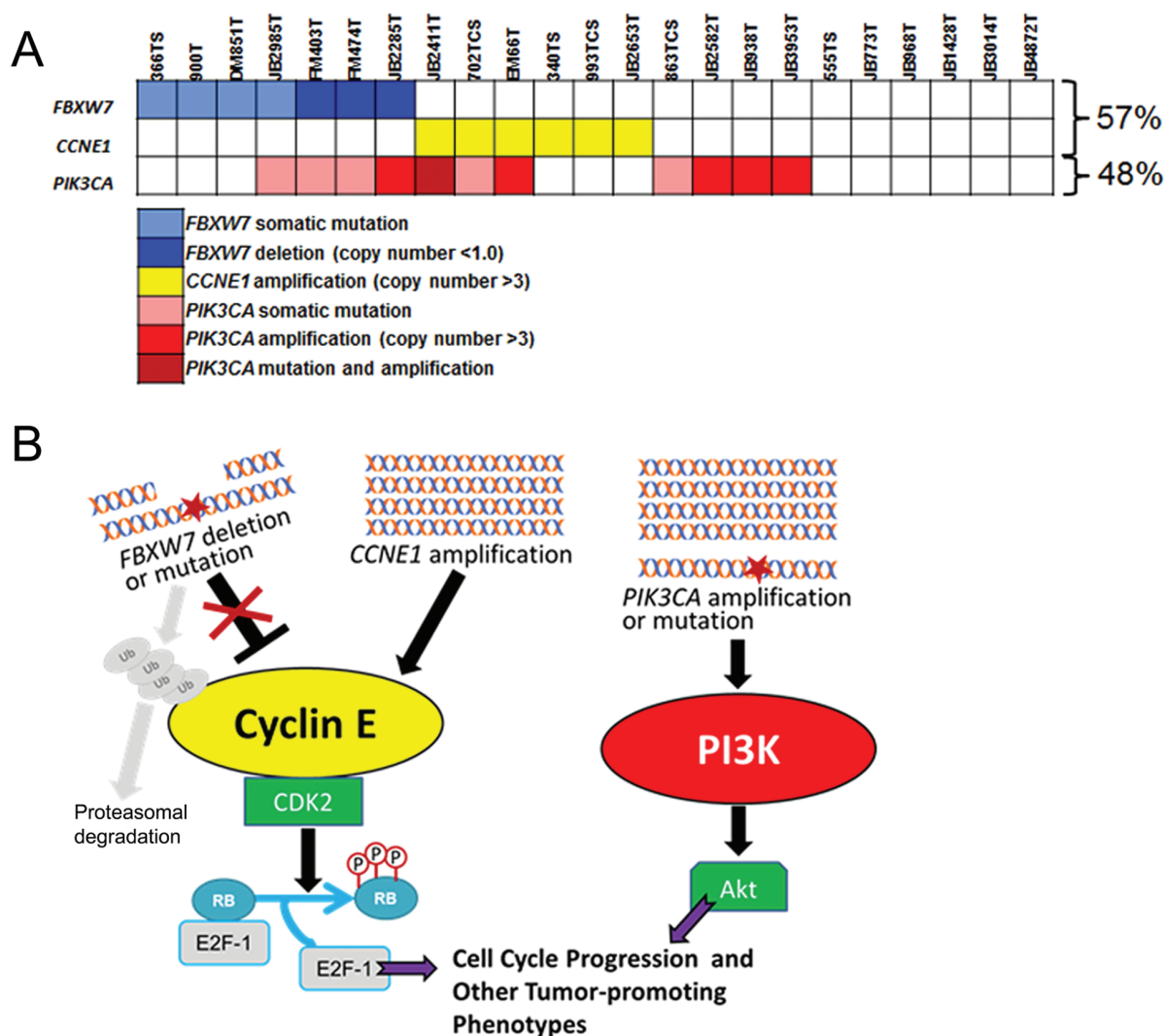


Figure 2. Molecular genetic alterations involving the FBXW7–cyclin E and phosphatidylinositol 3-kinase (PI3K) pathways in uterine serous carcinoma. **A**) Summary of sequence mutations and DNA copy number changes in *FBXW7*, *CCNE1*, and *PIK3CA*. **B**) Schematic presentation of possible mechanisms involving the FBXW7–cyclin E and PI3K pathways in the development of uterine serous carcinoma. *FBXW7* gene deletion or mutation results in an increased level of cyclin E because of the suppression of FBXW7-mediated ubiquitination and subsequent proteasome-mediated degradation of cyclin E proteins. Alternatively, activation of PI3K can be a result of increased DNA copy number of *PIK3CA* and activating mutation of the gene. Increased E2F-1 and PI3K activity leads to activation of their downstream targets that promote cell cycle progression and other tumor-promoting phenotypes. Ub = ubiquitin; P = phosphate.

***FBXW7*, *PIK3CA*, *PPP2R1A*, and *TP53* Mutations in Serous Endometrial Intraepithelial Carcinoma**

It has been proposed that serous endometrial intraepithelial carcinoma is the preinvasive precursor of uterine serous carcinoma (7,33,34). We, therefore, examined whether somatic mutations of the frequently mutated genes in uterine serous carcinoma identified in this study, including *FBXW7*, *PIK3CA*, *PPP2R1A*, and *TP53*, occurred in serous endometrial intraepithelial carcinoma. We identified nine uterine serous carcinomas that had a concurrent serous endometrial intraepithelial carcinoma component; we laser-capture microdissected nine serous endometrial intraepithelial carcinomas for mutation analysis. As summarized in Figure 3, A, all nine pairs of serous carcinoma and associated serous endometrial intraepithelial carcinoma had concordant *PIK3CA*, *PPP2R1A*, and *TP53* mutation status between uterine serous carcinoma and its concurrent serous endometrial intraepithelial carcinoma component, whereas eight

of the nine pairs had concordant *FBXW7* mutation status between these two components. The only discordant pair (case ID: 1FFPE) contained a *FBXW7* p.Asp440Asn mutation in the uterine serous carcinoma component, but this mutation was not detected in the serous endometrial intraepithelial carcinoma.

We also examined whether cyclin E protein expression, as detected by immunohistochemistry, was increased in *FBXW7* mutated serous endometrial intraepithelial carcinomas. We found that all four pairs of serous endometrial intraepithelial carcinomas and concurrent serous carcinomas with a *FBXW7* mutation had increased cyclin E expression compared with normal endometrial epithelium. The expression of cyclin E and *FBXW7* mutation status in one of the cases are shown in Figure 3, B. The locations of *FBXW7* mutations, including those found in five serous endometrial intraepithelial carcinomas and in 15 uterine serous carcinomas, are shown in Figure 3, C. All mutations were missense mutations

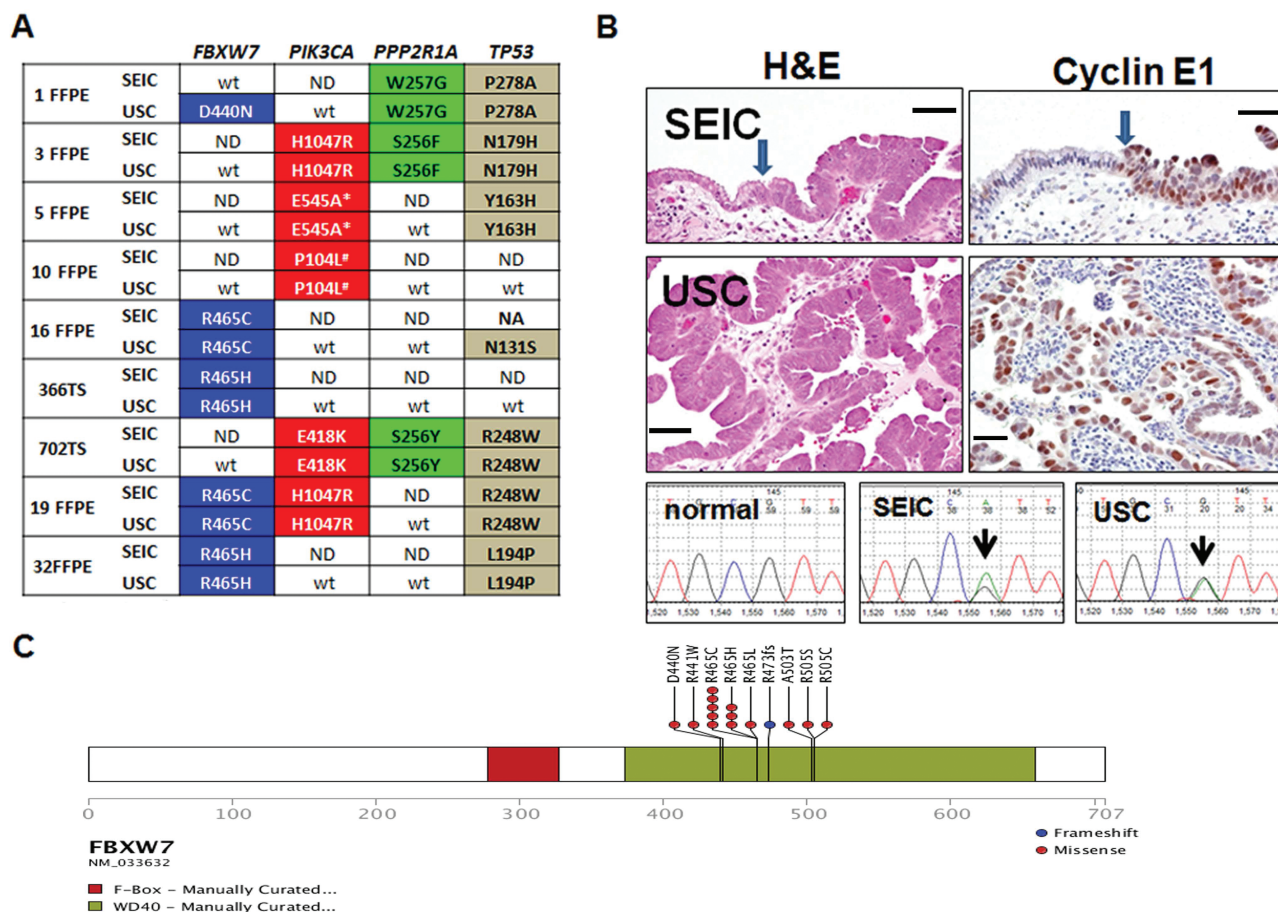


Figure 3. Mutation profiles of the most commonly mutated genes and cyclin E expression in uterine serous carcinoma (USC) and serous endometrial intraepithelial carcinoma (SEIC). **A)** Mutation profiles of *FBXW7*, *PIK3CA*, *PPP2R1A*, and *TP53* in nine USCs with a concurrent SEIC component. Manual microdissection and laser-capture microdissection were used to isolate USC and SEIC, respectively, for DNA analysis. Mutations are highlighted in different colors for each gene. ND = not done; wt = wildtype; NA = not available for analysis; *tumor (5FFPE) has two additional mutations in *PIK3CA*: S553Ifs, H1047R; #tumor (10FFPE) has one additional mutation in *PIK3CA*: G1007R. **B)** A uterine serous carcinoma with a serous endometrial intraepithelial carcinoma component. Top panel, SEIC; middle panel, USC. The tumor cells in both lesions show highly atypical and enlarged nuclei. The **arrow** indicates the junction between normal-appearing uterine surface epithelium (left) and serous endometrial intraepithelial carcinoma (right). Cyclin E immunoreactivity (**brown**) was detected in both uterine serous carcinoma and serous endometrial intraepithelial carcinoma cells but not in adjacent normal epithelium or stromal cells (scale bar = 100 μ m). Bottom panels: Mutational analysis showing an identical somatic mutation of *FBXW7*, from CGT to CAT (**arrows**), leading to the amino acid change R465H in both the serous endometrial intraepithelial carcinoma and the uterine serous carcinoma. **C)** Locations of *FBXW7* mutations identified among the 76 uterine serous carcinomas. Each **circle** represents an individual mutation.

except one (a splice site mutation) and were located in the WD40 domain. Our finding that most uterine serous carcinomas and their in situ counterparts have identical mutations, when taken together with previous reports (35,36) showing *TP53* mutations in serous endometrial intraepithelial carcinoma, indicates that mutations in *FBXW7*, *PIK3CA*, *PPP2R1A*, and *TP53* occur early during tumor progression of uterine serous carcinoma.

Discussion

This is the first study to our knowledge to characterize the genomic landscape of uterine serous carcinoma, a highly aggressive neoplastic disease in women. Whole-exome sequencing and DNA copy number analysis demonstrated that mutations in *TP53*, *PIK3CA*, and *FBXW7*, as well as amplification of *CCNE1*, are the most common genetic alterations in this type of tumor. The presence of *FBXW7* mutations and *CCNE1* amplification increased the levels

of cyclin E protein, which facilitates cell cycle progression through cdk2, Rb phosphorylation, and E2F-1 (Figure 2, B). Conversely, an activating mutation and/or gene amplification of *PIK3CA* would enhance PI3K signaling and, subsequently, Akt activity, which promotes cellular proliferation and survival (Figure 2, B). Therefore, both signaling pathways may work in concert to promote tumorigenesis in uterine serous carcinoma. Because patients with uterine serous carcinoma are often diagnosed at late clinical stages when conventional chemotherapy is not effective, there is an unmet need to develop new therapeutics for those patients. The results as reported here suggest that PI3K inhibitors and inhibitors targeting the cyclin E pathway may represent new therapeutic interventions in advanced-stage uterine serous carcinoma.

Our results also have several biological implications regarding the molecular genetics of uterine serous carcinoma. First, this study not only confirmed frequent *PIK3CA*, *PPP2R1A*, and *TP53* mutations in uterine serous carcinoma as previously reported (35,37–40)

but also identified novel recurrent somatic mutations of *FBXW7*, which occurred in approximately 20% of tumors. Although *FBXW7* mutations have been reported in several types of human cancers, including those of hematopoietic, gastrointestinal tract, pancreatic, uterine, and cervical origins (41), to our knowledge, this gene has not been sequenced in uterine serous carcinoma. *FBXW7*, also known as *bCDC4*, is a member of the F-box family of proteins that serves as a substrate recognition component of the ubiquitin ligase SCF complex (41,42). *FBXW7* functions as a haploinsufficient tumor suppressor gene (43), and the protein is responsible for the ubiquitin-dependent proteolysis of several tumor-promoting proteins, including cyclin E, c-Jun, c-Myc, MCL1, and Notch (42,44–48). It is interesting that our DNA copy number analysis revealed that the *CCNE1* locus is one of the most frequently amplified chromosomal regions in uterine serous carcinoma and that *CCNE1* amplification occurs mutually exclusively with *FBXW7* mutations (including point mutation and deletion), suggesting that *CCNE1* and *FBXW7* participate in the same signaling pathway. In fact, we found that molecular genetic aberrations in the cyclin E pathway due to *FBXW7* point mutations, *FBXW7* deletions, or *CCNE1* amplification, when considered together, occurred in more than half of uterine serous carcinomas. Thus, activation of cyclin E, either by inhibiting its ubiquitin-dependent protein degradation due to *FBXW7* mutations or by increased expression as a result of gene amplification, may play a major role in driving the tumorigenesis of uterine serous carcinoma.

Second, we observed that concordant mutation status in *PIK3CA*, *PPP2R1A*, and *TP53* occurred in all nine pairs of tumors containing uterine serous carcinoma and concurrent serous endometrial intraepithelial carcinoma, whereas concordant *FBXW7* mutation status was found in eight of nine pairs. This result suggests that mutations of the above genes occurred in the preinvasive stage of uterine serous carcinoma and, if confirmed in a larger number of tumors, may have translational implications. For example, detection of those mutations may be helpful for screening for uterine serous carcinoma at a preinvasive stage in endometrial curettage or cervical lavage specimens using emerging highly sensitive molecular techniques.

Third, our results may clarify the relationship between uterine serous carcinoma and ovarian high-grade serous carcinoma, another highly aggressive gynecologic neoplasm. These two tumors have different clinicopathologic features, such as older age at diagnosis for uterine serous carcinoma compared with ovarian high-grade serous carcinoma [68 years for uterine serous carcinoma vs 55 years for ovarian high-grade serous carcinoma (7)] and a genetic predisposition for some cases of ovarian serous carcinoma due to germline *BRCA1* and *BRCA2* mutations (7) but not for uterine serous carcinoma. However, uterine serous carcinoma and ovarian high-grade serous carcinoma have some similar features, including an aggressive clinical course, certain morphological features, and a similar relationship to intraepithelial carcinoma precursors (7). Molecularly, both are characterized by a high prevalence of *TP53* mutations, a similar overall number of somatic mutations, and a high level of genome-wide DNA copy number alterations. In fact, in the World Health Organization histopathologic classification (6,49), the term “serous carcinoma” is used to describe both tumors, implying that they share similar morphological features. However, in this study, we

found a higher frequency of somatic mutations in *FBXW7*, *PIK3CA*, and *PPP2R1A* in uterine serous carcinoma compared with ovarian high-grade serous carcinoma, providing evidence for molecular genetic alterations that are unique to uterine serous carcinoma.

There are two major limitations in this study. First, we focused on only 10 uterine serous carcinomas in the discovery set, and it is possible that other somatic genetic changes will be identified in studies using a larger cohort. Second, we did not investigate whether the molecular changes reported here are associated with any clinical features. Therefore, it will be interesting to determine whether mutations in *FBXW7*, *PIK3CA*, *PPP2R1A*, or *TP53* are associated with clinical stage, disease-free or overall survival, or response to treatment.

In summary, genome-wide analyses identified aberrations involving three pathways, the p53, PI3K, and cyclin E–FBXW7 pathways, in uterine serous carcinomas. Our findings have important implications not only for understanding the pathogenesis of uterine serous carcinoma but possibly also for developing more effective target-based therapy. Moreover, the presence of these changes in the preinvasive stage of uterine serous carcinoma suggests that these molecular alterations occur relatively early in tumor progression and may serve as molecular markers for early detection of uterine serous carcinoma.

References

1. American Cancer Society. *Cancer Facts & Figures 2012*. Atlanta: American Cancer Society; 2012.
2. Bokhman JV. Two pathogenetic types of endometrial carcinoma. *Gynecol Oncol*. 1983;15(1):10–17.
3. Hamilton CA, Cheung MK, Osann K, et al. Uterine papillary serous and clear cell carcinomas predict for poorer survival compared to grade 3 endometrioid corpus cancers. *Br J Cancer*. 2006;94(5):642–646.
4. Di Cristofano A, Ellenson LH. Endometrial carcinoma. *Annu Rev Pathol*. 2007;2:57–85.
5. Guan B, Mao TL, Panuganti PK, et al. Mutation and loss of expression of ARID1A in uterine low-grade endometrioid carcinoma. *Am J Surg Pathol*. 2011;35(5):625–632.
6. Silverberg SG, Mutter GL, Kurman RJ, Kubik-Huch RA, Nogales F, Tavassoli FA. Tumors of uterine corpus. In: Tavassoli FA, Devilee P, eds. *Pathology and Genetics: Tumors of the Breast and Female Genital Organs, WHO Classification of Tumors*. Lyon, France: IARC Press; 2003:217–257.
7. Ellenson LH, Ronnett BM, Soslow RA, Zaino RJ, Kurman RJ. Endometrial carcinoma. In: Kurman RJ, Ellenson LH, Ronnett BM, eds. *Blaustein's Pathology of the Female Genital Tract*. 6th ed. New York, NY: Springer; 2011:393–452.
8. Jones S, Wang TL, Shih IeM, et al. Frequent mutations of chromatin remodeling gene ARID1A in ovarian clear cell carcinoma. *Science*. 2010;330(6001):228–231.
9. Jones S, Wang TL, Kurman RJ, et al. Low-grade serous carcinomas of the ovary contain very few point mutations. *J Pathol*. 2012;226(3):413–420.
10. Li H, Durbin R. Fast and accurate short read alignment with Burrows-Wheeler transform. *Bioinformatics*. 2009;25(14):1754–1760.
11. Edmonson MN, Zhang J, Yan C, Finney RP, Meerzaman DM, Buetow KH. Bambino: a variant detector and alignment viewer for next-generation sequencing data in the SAM/BAM format. *Bioinformatics*. 2011;27(6):865–866.
12. Pruitt KD, Tatusova T, Klimke W, Maglott DR. NCBI Reference Sequences: current status, policy and new initiatives. *Nucleic Acids Res*. 2009;37(Database issue):D32–6.
13. Zhang J, Ding L, Holmfeldt L, et al. The genetic basis of early T-cell precursor acute lymphoblastic leukaemia. *Nature*. 2012;481(7380):157–163.
14. Zhang J, Benavente CA, McEvoy J, et al. A novel retinoblastoma therapy from genomic and epigenetic analyses. *Nature*. 2012;481(7381):329–334.

15. Cancer Genome Research Atlas Network. Comprehensive genomic characterization defines human glioblastoma genes and core pathways. *Nature*. 2008;455(7216):1061–1068.
16. Kuo KT, Mao TL, Chen X, et al. DNA copy number profiles in affinity-purified ovarian clear cell carcinoma. *Clin Cancer Res*. 2010;16(7):1997–2008.
17. Kuo KT, Guan B, Feng Y, et al. Analysis of DNA copy number alterations in ovarian serous tumors identifies new molecular genetic changes in low-grade and high-grade carcinomas. *Cancer Res*. 2009;69(9):4036–4042.
18. Olshen AB, Venkatraman ES, Lucito R, Wigler M. Circular binary segmentation for the analysis of array-based DNA copy number data. *Biostatistics*. 2004;5(4):557–572.
19. Venkatraman ES, Olshen AB. A faster circular binary segmentation algorithm for the analysis of array CGH data. *Bioinformatics*. 2007;23(6):657–663.
20. Beroukhi R, Getz G, Nghiemphu L, et al. Assessing the significance of chromosomal aberrations in cancer: methodology and application to glioma. *Proc Natl Acad Sci U S A*. 2007;104(50):20007–20012.
21. Kuhn E, Kurman RJ, Vang R, et al. TP53 mutations in serous tubal intraepithelial carcinoma and concurrent pelvic high-grade serous carcinoma—evidence supporting the clonal relationship of the two lesions. *J Pathol*. 2012;226(3):421–426.
22. The Cancer Genome Atlas Research Network. Integrated genomic analyses of ovarian carcinoma. *Nature*. 2011;474(7353):609–615.
23. Calhoun ES, Jones JB, Ashfaq R, et al. BRAF and FBXW7 (CDC4, FBW7, AGO, SEL10) mutations in distinct subsets of pancreatic cancer: potential therapeutic targets. *Am J Pathol*. 2003;163(4):1255–1260.
24. Samuels Y, Wang Z, Bardelli, et al. High frequency of mutations of the PIK3CA gene in human cancers. *Science*. 2004;304(5670):554.
25. Jones S, Wang TL, Shih IeM, et al. Frequent mutations of chromatin remodeling gene ARID1A in ovarian clear cell carcinoma. *Science*. 2010;330(6001):228–231.
26. Fortier JM, Kornbluth J. NK lytic-associated molecule, involved in NK cytotoxic function, is an E3 ligase. *J Immunol*. 2006;176(11):6454–6463.
27. Ambrose EC, Kornbluth J. Downregulation of uridine-cytidine kinase like-1 decreases proliferation and enhances tumor susceptibility to lysis by apoptotic agents and natural killer cells. *Apoptosis*. 2009;14(10):1227–1236.
28. Kashuba E, Kashuba V, Sandalova T, Klein G, Szekely L. Epstein-Barr virus encoded nuclear protein EBNA-3 binds a novel human uridine kinase/uracil phosphoribosyltransferase. *BMC Cell Biol*. 2002;3(8):23.
29. Okabe H, Lee SH, Phuchareon J, Albertson DG, McCormick F, Tetsu O. A critical role for FBXW7 and MAPK in cyclin D1 degradation and cancer cell proliferation. *PLoS One*. 2006;1(1):e128.
30. Foster FM, Traer CJ, Abraham SM, Fry MJ. The phosphoinositide (PI) 3-kinase family. *J Cell Sci*. 2003;116(15):3037–3040.
31. Pickart CM. Mechanisms underlying ubiquitination. *Annu Rev Biochem*. 2001;70:503–533.
32. Rajagopalan H, Nowak MA, Vogelstein B, Lengauer C. The significance of unstable chromosomes in colorectal cancer. *Nat Rev Cancer*. 2003;3(9):695–701.
33. Ambros RA, Sherman ME, Zahn CM, Bitterman P, Kurman RJ. Endometrial intraepithelial carcinoma: a distinctive lesion specifically associated with tumors displaying serous differentiation. *Hum Pathol*. 1995;26(11):1260–1267.
34. Sherman ME, Bur ME, Kurman RJ. p53 in endometrial cancer and its putative precursors: evidence for diverse pathways of tumorigenesis. *Hum Pathol*. 1995;26(11):1268–1274.
35. Tashiro H, Isacson C, Levine R, Kurman RJ, Cho KR, Hedrick L. p53 gene mutations are common in uterine serous carcinoma and occur early in their pathogenesis. *Am J Pathol*. 1997;150(1):177–185.
36. Baergen RN, Warren CD, Isacson C, Ellenson LH. Early uterine serous carcinoma: clonal origin of extrauterine disease. *Int J Gynecol Pathol*. 2001;20(3):214–219.
37. Lax SF, Kendall B, Tashiro H, Slebos RJ, Hedrick L. The frequency of p53, K-ras mutations, and microsatellite instability differs in uterine endometrioid and serous carcinoma: evidence of distinct molecular genetic pathways. *Cancer*. 2000;88(4):814–824.
38. Kovalev S, Marchenko ND, Gugliotta BG, Chalas E, Chumas J, Moll UM. Loss of p53 function in uterine papillary serous carcinoma. *Hum Pathol*. 1998;29(6):613–619.
39. Hayes MP, Douglas W, Ellenson LH. Molecular alterations of EGFR and PIK3CA in uterine serous carcinoma. *Gynecol Oncol*. 2009;113(3):370–373.
40. Shih IeM, Wang TL. Mutation of PPP2R1A: a new clue in unveiling the pathogenesis of uterine serous carcinoma. *J Pathol*. 2011;224(1):1–4.
41. Welcker M, Clurman BE. FBW7 ubiquitin ligase: a tumour suppressor at the crossroads of cell division, growth and differentiation. *Nat Rev Cancer*. 2008;8(2):83–93.
42. Onoyama I, Nakayama KI. Fbxw7 in cell cycle exit and stem cell maintenance: insight from gene-targeted mice. *Cell Cycle*. 2008;7(21):3307–3313.
43. Sancho R, Jandke A, Davis H, Diefenbacher ME, Tomlinson I, Behrens A. F-box and WD repeat domain-containing 7 regulates intestinal cell lineage commitment and is a haploinsufficient tumor suppressor. *Gastroenterology*. 2010;139(3):929–941.
44. Onoyama I, Tsunematsu R, Matsumoto A, et al. Conditional inactivation of Fbxw7 impairs cell-cycle exit during T cell differentiation and results in lymphomagenesis. *J Exp Med*. 2007;204(12):2875–2888.
45. Tan Y, Sangfelt O, Spruck C. The Fbxw7/hCdc4 tumor suppressor in human cancer. *Cancer Lett*. 2008;271(1):1–12.
46. Akhond S, Sun D, Lehr von der N, et al. FBXW7/hCDC4 is a general tumor suppressor in human cancer. *Cancer Res*. 2007;67(19):9006–9012.
47. Wertz IE, Kusam S, Lam C, et al. Sensitivity to antitubulin chemotherapeutics is regulated by MCL1 and FBW7. *Nature*. 2011;471(7336):110–114.
48. Tetzlaff MT, Yu W, Li M, et al. Defective cardiovascular development and elevated cyclin E and Notch proteins in mice lacking the Fbw7 F-box protein. *Proc Natl Acad Sci U S A*. 2004;101(10):3338–3345.
49. Lee KR, Russell P, Tavassoli FA, et al. Tumors of the ovary and peritoneum-surface epithelial-stromal tumors. In: Tavassoli FA, Devilee P, eds. *Pathology and Genetics: Tumors of the Breast and Female Genital Organs, WHO Classification of Tumors*. Lyon, France: IARC Press; 2003:113–202.

Funding

This work was supported by the National Cancer Institute at the National Institutes of Health (RO1 CA103937, RO1 CA129080, RO1 CA148826, RO1 CA122581, P50 CA098252), the National Taiwan University Hospital (NTUH98-1265), and the National Science Council in Taiwan (NSC99-2320-B-002-056-MY2).

Notes

EK, R-CW, GW, and BG contributed equally to this work. The authors declare no conflict of interest. The funders did not have any involvement in the design of the study; the collection, analysis, and interpretation of the data; the writing of the article; or the decision to submit the article for publication.

Affiliations of Authors: Departments of Pathology, Oncology, and Gynecology/Obstetrics, Johns Hopkins Medical Institutions, Baltimore, MD (EK, R-CW, BG, RBR, RJK, T-LW, I-MS); St. Jude Children's Research Hospital, Memphis, TN (GW, JZ, LW); Bradley Department of Electrical and Computer Engineering, Virginia Polytechnic Institute and State University, Blacksburg, VA (YW, LS, XY); Department of Pathology, National Taiwan University Hospital, Medical College, National Taiwan University, Taipei, Taiwan (K-TK); Shimane University, Japan (KN); Department of Pathology, Toronto Health Care system, Toronto, ON, Canada (BC, PS); Department of Pathology, Chang Gung Memorial Hospital and Chang Gung University College of Medicine, Taoyuan, Taiwan (R-CW); Department of Surgery, Memorial Sloan-Kettering Cancer Center, New York, NY (NO, DAL).